INTERNATIONAL JOURNAL OF CIRCUIT THEORY AND APPLICATIONS
Int. J. Circ. Theor. Appl. 2011; **39**:589–606
Published online 29 April 2010 in Wiley Online Library (wileyonlinelibrary.com). DOI: 10.1002/cta.664

Pathological representation of the two-output CCII and ICCII family and application

Ahmed M. Soliman*, †

Electronics and Communications Engineering Department, Faculty of Engineering Cairo University, Giza 12613, Egypt

SUMMARY

The pathological mirror and nullor representation of the two-output current conveyor family is given. New pathological mirror and nullor representations of the two-output current conveyor family are given and compared with the corresponding nullator norator resistors' realizations. Simplified representations of the two-output current conveyors based on using two single-output current conveyors are given. Two examples are given, the first example demonstrates the importance of the pathological representation in the generation of a family of 16 oscillators from a two-output current conveyor-based current mode oscillator. A second example of a current mode low-pass filter using two single-output inverting current conveyors is considered. Its simplified modeling using a single balanced output inverting current conveyor is compared with the original current mode filter and the simulation results are given. Copyright © 2010 John Wiley & Sons, Ltd.

Received 24 March 2009; Revised 11 October 2009; Accepted 6 December 2009

KEY WORDS: pathological VM; pathological CM; nullator; norator; two-output current conveyor family; current mode low-pass filter

1. INTRODUCTION

The nullator norator [1] representation of active building blocks is an important topic as it leads to alternative equivalent realizations. It is well known that the nullator norator combinations cannot realize the CCII+ unless additional resistors are used as demonstrated in [2, 3]. The inverting current conveyor (ICCII) was introduced in [4] to complete the single-output CCII family. The two members of the single-output ICCII are the ICCII− and the ICCII+. The nullator and the norator cannot realize the ICCII− nor can they realize the ICCII+ unless additional resistors are used. The pathological voltage mirror (VM) and the pathological current mirror (CM) introduced in [4, 5] provided means of representing the four single-output CCII and ICCII members without any need to use resistors [4].The systematic synthesis of active circuits developed in [6, 7] is based on using the nullor elements and the basic ideas were extended in [8, 9] to accommodate the pathological mirror elements to allow more ideal representations of active circuits.

The two-output current conveyors were introduced in the literature in [10, 11] to allow the active circuit to provide an output current from a high impedance node namely the additional Z terminal of the two-output current conveyor. The pathological representation of the two-output current conveyor family is given in details in this paper to provide complete models allowing for complete generation of ideal equivalent active circuits and oscillators.

*Correspondence to: Ahmed M. Soliman, Electronics and Communications Engineering Department, Faculty of Engineering Cairo University, Giza 12613, Egypt.
†E-mail: asoliman@ieee.org

2. PATHOLOGICAL REPRESENTATION OF TWO-OUTPUT CCII AND ICCII FAMILY

The two-output CCII family includes three members namely the balanced output CCII (BOCCII), the double output CCII with two $Z+$ outputs (DOCCII$++$) and the double output CCII with two $Z-$ outputs (DOCCII$--$). The symbol and the matrix equation defining each of the three types are given in Table I. The magnitude of the current in the ground terminal I_G in terms of I_X is also included in Table I.

The two-output ICCII family includes three members namely the balanced output ICCII (BOICCII), the double output ICCII with two $Z+$ outputs (DOICCII$++$) and the double output ICCII with two $Z-$ outputs (DOICCII$--$). The symbol and the matrix equation defining each of the three types are given in Table II. The magnitude of the current in the ground terminal I_G in terms of I_X is also included in Table II.

Very recently modeling of the two-output CCII has been described in the literature [12, 13]. The two-output CCII is modeled in [12] using one nullator, one norator and two current-controlled current sources (CCCS) as a special case from a multiple output CCII. The BOCCII is modeled in [13] using four nullators, four norators and five grounded resistors. Although the well-known representation of the ICCII$-$ given in [4]—using two nullators, two norators and two grounded resistors is described in [13], no nullator norator representations for the two-output ICCII is given in [13] or in [12].

Table I. The two-output CCII family members.

Two-output CCII	Symbol	Equation
Balanced output CCII	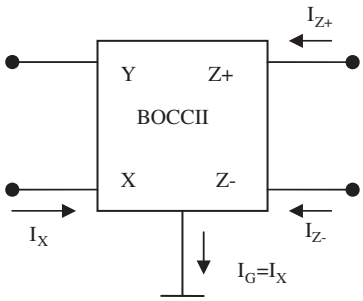	$\begin{bmatrix} V_X \\ I_Y \\ I_{Z+} \\ I_{Z-} \end{bmatrix} = \begin{bmatrix} 0 & 1 & 0 & 0 \\ 0 & 0 & 0 & 0 \\ 1 & 0 & 0 & 0 \\ -1 & 0 & 0 & 0 \end{bmatrix} \begin{bmatrix} I_X \\ V_Y \\ V_{Z+} \\ V_{Z-} \end{bmatrix}$
Double output CCII$++$	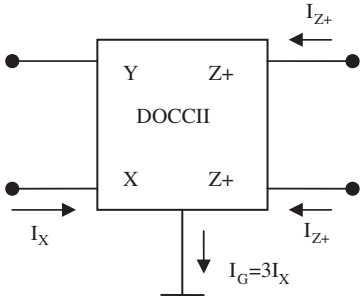	$\begin{bmatrix} V_X \\ I_Y \\ I_{Z+} \\ I_{Z+} \end{bmatrix} = \begin{bmatrix} 0 & 1 & 0 & 0 \\ 0 & 0 & 0 & 0 \\ 1 & 0 & 0 & 0 \\ 1 & 0 & 0 & 0 \end{bmatrix} \begin{bmatrix} I_X \\ V_Y \\ V_{Z+} \\ V_{Z+} \end{bmatrix}$
Double output CCII$--$	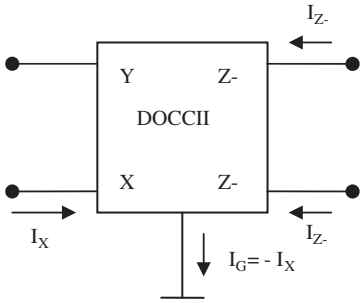	$\begin{bmatrix} V_X \\ I_Y \\ I_{Z-} \\ I_{Z-} \end{bmatrix} = \begin{bmatrix} 0 & 1 & 0 & 0 \\ 0 & 0 & 0 & 0 \\ -1 & 0 & 0 & 0 \\ -1 & 0 & 0 & 0 \end{bmatrix} \begin{bmatrix} I_X \\ V_Y \\ V_{Z-} \\ V_{Z-} \end{bmatrix}$

DOI: 10.1002/cta

Table II. The two-output ICCII family members.

Two-output ICCII	Symbol	Equation
Balanced output ICCII	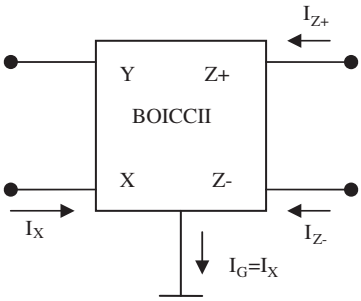	$\begin{bmatrix} V_X \\ I_Y \\ I_{Z+} \\ I_{Z-} \end{bmatrix} = \begin{bmatrix} 0 & -1 & 0 & 0 \\ 0 & 0 & 0 & 0 \\ 1 & 0 & 0 & 0 \\ -1 & 0 & 0 & 0 \end{bmatrix} \begin{bmatrix} I_X \\ V_Y \\ V_{Z+} \\ V_{Z-} \end{bmatrix}$
Double output ICCII++	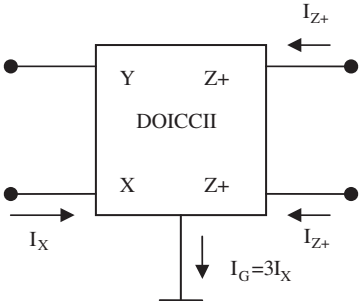	$\begin{bmatrix} V_X \\ I_Y \\ I_{Z+} \\ I_{Z+} \end{bmatrix} = \begin{bmatrix} 0 & -1 & 0 & 0 \\ 0 & 0 & 0 & 0 \\ 1 & 0 & 0 & 0 \\ 1 & 0 & 0 & 0 \end{bmatrix} \begin{bmatrix} I_X \\ V_Y \\ V_{Z+} \\ V_{Z+} \end{bmatrix}$
Double output ICCII−−	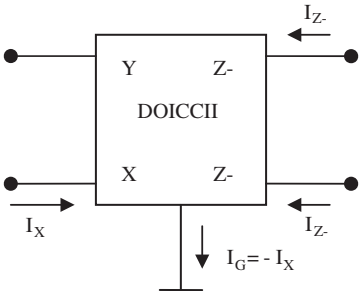	$\begin{bmatrix} V_X \\ I_Y \\ I_{Z-} \\ I_{Z-} \end{bmatrix} = \begin{bmatrix} 0 & -1 & 0 & 0 \\ 0 & 0 & 0 & 0 \\ -1 & 0 & 0 & 0 \\ -1 & 0 & 0 & 0 \end{bmatrix} \begin{bmatrix} I_X \\ V_Y \\ V_{Z-} \\ V_{Z-} \end{bmatrix}$

From the above brief review it is clear that the pathological representation of the two-output CCII and ICCII family needs to be completed.

Before considering the nullor mirror pathological representation, it is important to point out that for a physical realization of the circuit the total number of nullators plus the number of VM must equal to the number of norators plus the number of CM as explained in [4, 9].

Most recently the pathological representation of the BOCCII using two nullators and two CM and no resistors was given in [9] and is shown here in Figure 1(a). Figure 1(b) represents a new pathological representation of the DOCCII++ using three CM and three nullators. It should be noted that one of the nullators is dummy and is included to have equal number of nullators and CM as explained above. Figure 1(c) represents a new pathological representation of the DOCCII−− using two CM and two nullators.

It is clear that in each of the above three realizations, the grounded current I_G is given by I_X, $3I_X$ and $-I_X$, respectively, as given in Table I.

Figure 2(a) represents a new pathological representation of the BOICCII using one VM, one nullator and two CM. Figure 2(b) represents a new pathological representation of the BOICCII++ using one VM, two nullators and three CM. Figure 2(c) represents a new pathological representation of the DOICCII−− using one VM, one nullator and two CM. It is clear that in each of the above three realizations, the grounded current I_G is given by I_X, $3I_X$ and $-I_X$, respectively, as described in Table II.

DOI: 10.1002/cta

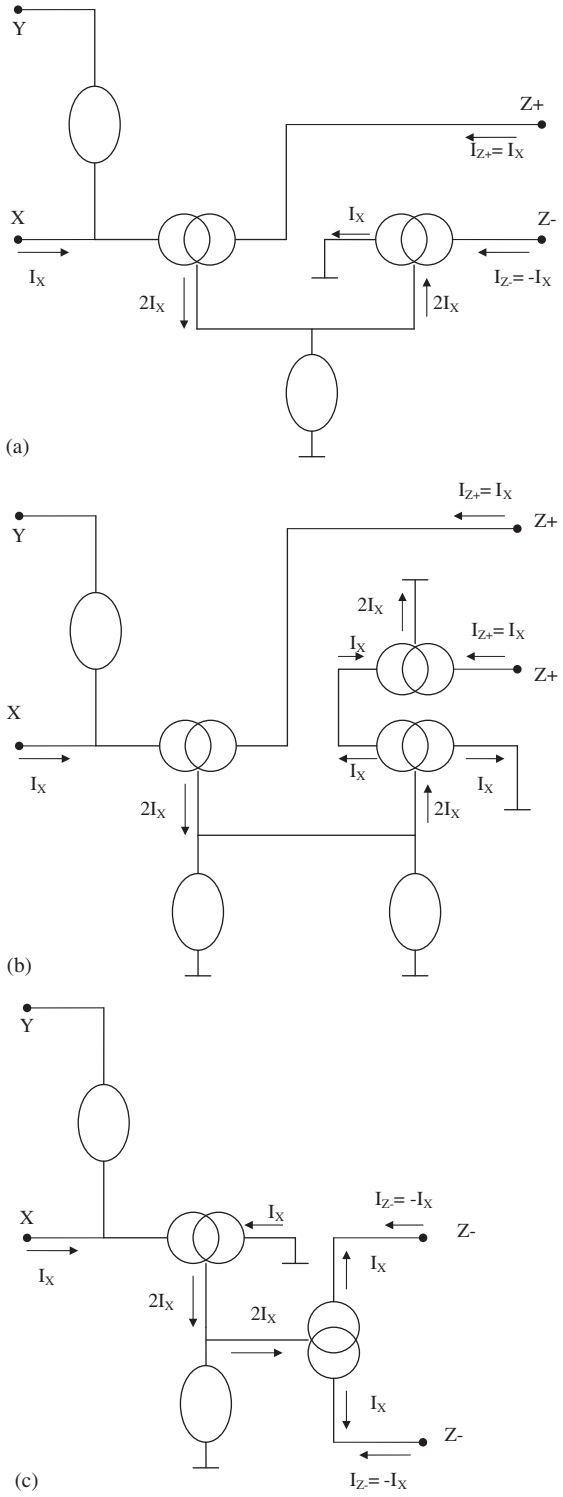

Figure 1. (a) Pathological element representation of the BOCCII [9]; (b) pathological element representation of the DOCCII++; and (c) pathological element representation of the DOCCII−−.

DOI: 10.1002/cta

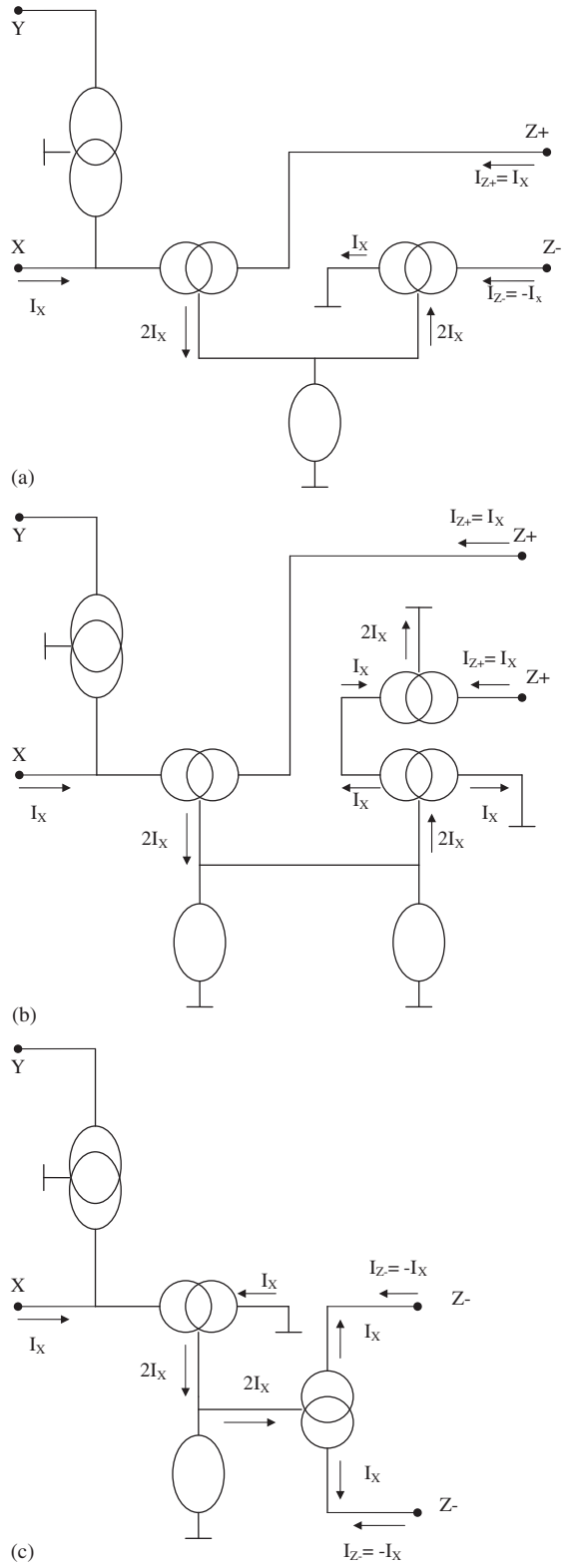

Figure 2. (a) Pathological element representation of the BOICCII; (b) pathological element representation of the DOICCII++; and (c) pathological element representation of the DOICCII−−.

DOI: 10.1002/cta

3. SIMPLIFIED REPRESENTATION OF TWO-OUTPUT CCII AND ICCII FAMILY

In this section a simplified pathological representation of the two-output CCII and ICCII family members is given based on an equivalent single-output CCII circuit. Each of the two-output CCII (or ICCII) can be represented by an equivalent two single-output CCII with a common Y input and in this case this composite CCII (or ICCII) will have two X terminals. Each of the two X input terminals will be connected to the same external resistor, which is originally connected to the X terminal of the two-output CCII (or ICCII). This composite CCII will be defined as a two X CCII (TXCCII). This is different from the differential X used in [14, 15]. The two X CCII, however, was used in [16] in the generation of a DOCCII++ from two single-output CCII+.

The symbolic representation of each of the two X, two-output CCII as well as the matrix representing the definition is given in Table III. It is worth noting that the two X terminals are for two single-output CCII and is shown in a symbolic form in Table III for compactness of the symbol.

Table IV represents the TXBOCCII realized from a CCII+ and a CCII− with a common Y terminal. In this realization, the current I_G is given by $2I_X$. The TXDOCCII++ realized from two, CCII+, with a common Y terminal is also given in Table IV. In this realization, the current I_G is given by $4I_X$. The TXDOCCII−− realized from two CCII− with a common Y terminal is also given in Table IV. In this realization, the current $I_G = 0$ and it is seen that this results in the property of having floating realization of the TXDOCCII−−, which is not possible to obtain with the single X DOCCII−− realization.

Table III. Two X two-output CCII family members.

Two X two-output CCII	Symbol	Equation
TX balanced output CCII	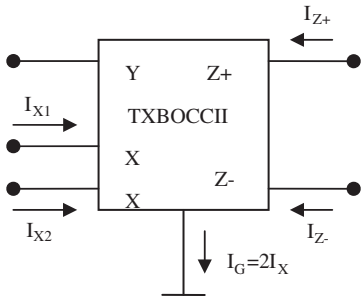	$\begin{bmatrix} V_{X1} \\ V_{X2} \\ I_Y \\ I_{Z+} \\ I_{Z-} \end{bmatrix} = \begin{bmatrix} 0 & 0 & 1 & 0 & 0 \\ 0 & 0 & 1 & 0 & 0 \\ 0 & 0 & 0 & 0 & 0 \\ 1 & 0 & 0 & 0 & 0 \\ 0 & -1 & 0 & 0 & 0 \end{bmatrix} \begin{bmatrix} I_{X1} \\ I_{x2} \\ V_Y \\ V_{Z+} \\ V_{Z-} \end{bmatrix}$
TX double output CCII++	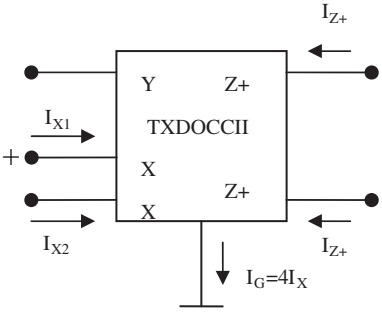	$\begin{bmatrix} V_{X1} \\ V_{X2} \\ I_Y \\ I_{Z+} \\ I_{Z+} \end{bmatrix} = \begin{bmatrix} 0 & 0 & 1 & 0 & 0 \\ 0 & 0 & 1 & 0 & 0 \\ 0 & 0 & 0 & 0 & 0 \\ 1 & 0 & 0 & 0 & 0 \\ 0 & 1 & 0 & 0 & 0 \end{bmatrix} \begin{bmatrix} I_{X1} \\ I_{x2} \\ V_Y \\ V_{Z+} \\ V_{Z+} \end{bmatrix}$
TX double output CCII−− (Floating)	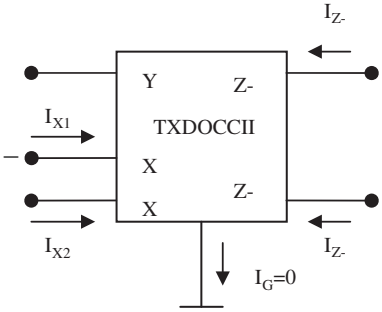	$\begin{bmatrix} V_{X1} \\ V_{X2} \\ I_Y \\ I_{Z-} \\ I_{Z-} \end{bmatrix} = \begin{bmatrix} 0 & 0 & 1 & 0 & 0 \\ 0 & 0 & 1 & 0 & 0 \\ 0 & 0 & 0 & 0 & 0 \\ -1 & 0 & 0 & 0 & 0 \\ 0 & -1 & 0 & 0 & 0 \end{bmatrix} \begin{bmatrix} I_{X1} \\ I_{x2} \\ V_Y \\ V_{Z+} \\ V_{Z-} \end{bmatrix}$

DOI: 10.1002/cta

Table IV. Realization of two X two-output CCII family members using two single-output CCII.

TX two-output CCII	Block diagram realization using two single-output CCII
TXBOCCII using a CCII+ and a CCII−	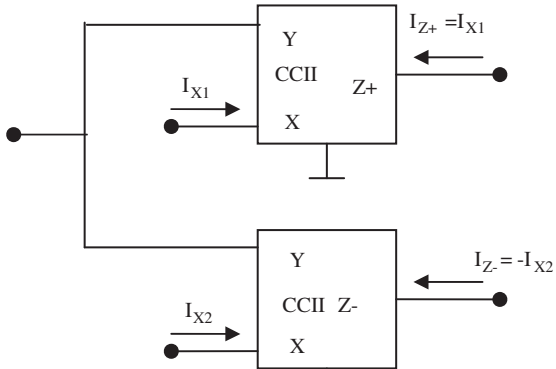
TXDOCCII++ using two CCII+	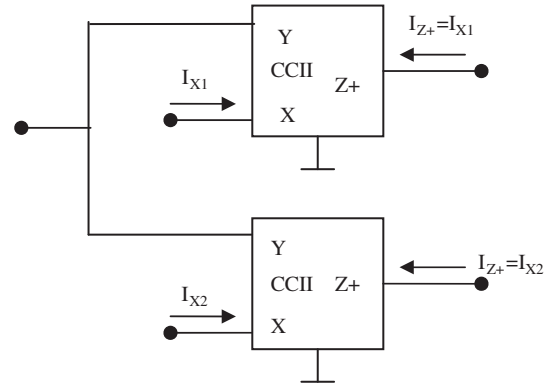
TXDOCCII−− using two CCII−	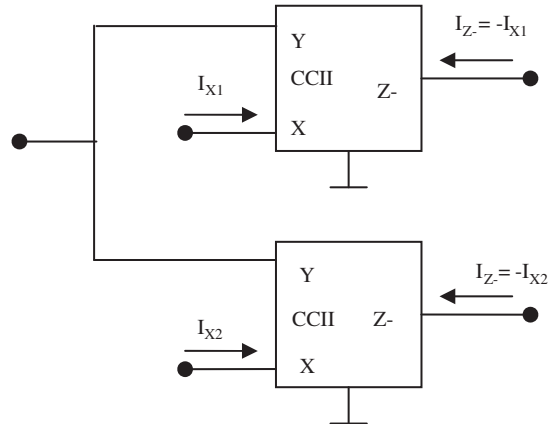

Figure 3(a) represents the new pathological representation of the TXBOCCII, which includes two nullators, one norator and one CM. It is clear that the two I_X currents are equal by using equal R_X resistors at both X ports and are marked as I_{X1} and I_{X2} just for clarification purposes. The current $I_G=2I_X$.

Figure 3(b) represents the new pathological representation of the TXDOCCII++, which includes two nullators and two CM, the current $I_G=4I_X$.

Figure 3(c) represents the new pathological representation of the floating TXDOCCII−−, which includes two nullators and two norators only, the current $I_G=0$.

The symbolic representation of each of the two X two-output ICCII as well as the matrix representing the definition is given in Table V.

DOI: 10.1002/cta

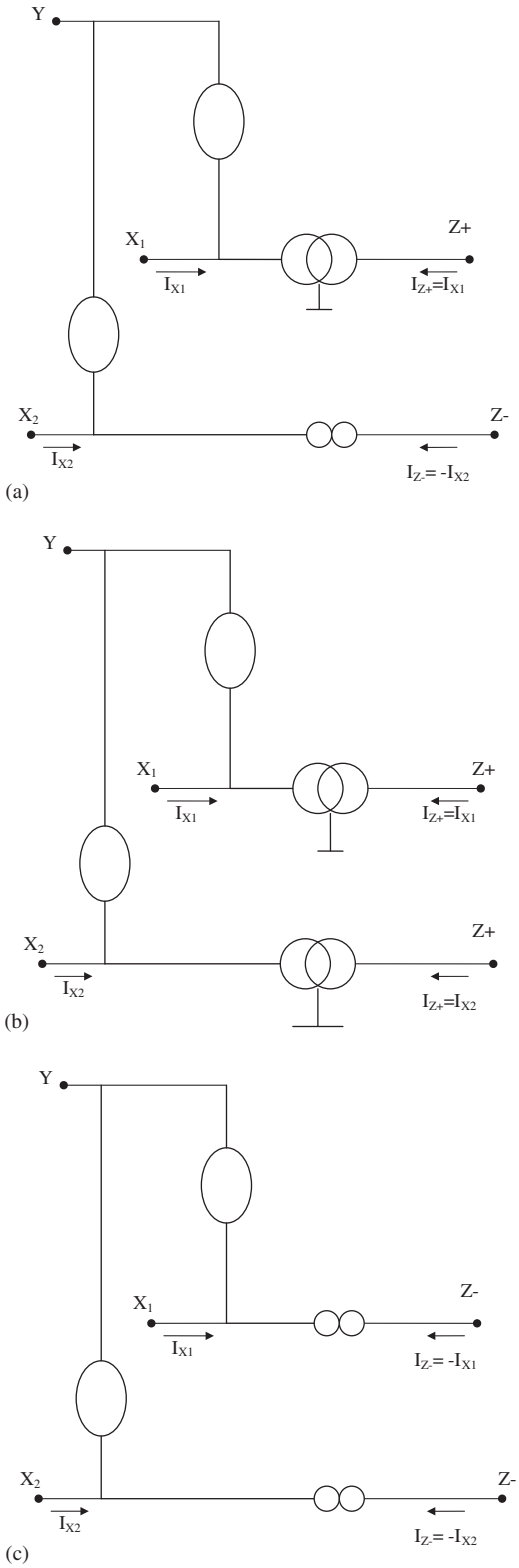

Figure 3. (a) Pathological representation of two X balanced output CCII; (b) pathological representation of two X DOCCII$++$; and (c) pathological representation of two X DOCCII$--$.

DOI: 10.1002/cta

Table V. Two *X* two-output ICCII family members.

Two *X* two-output ICCII	Symbol	Equation
TX balanced output ICCII	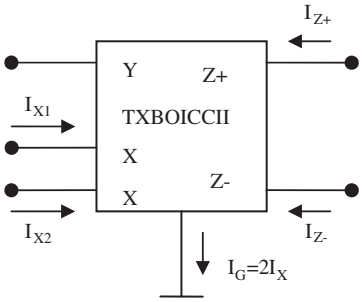	$\begin{bmatrix} V_{X1} \\ V_{X2} \\ I_Y \\ I_{Z+} \\ I_{Z-} \end{bmatrix} = \begin{bmatrix} 0 & 0 & -1 & 0 & 0 \\ 0 & 0 & -1 & 0 & 0 \\ 0 & 0 & 0 & 0 & 0 \\ 1 & 0 & 0 & 0 & 0 \\ 0 & -1 & 0 & 0 & 0 \end{bmatrix} \begin{bmatrix} I_{X1} \\ I_{x2} \\ V_Y \\ V_{Z+} \\ V_{Z-} \end{bmatrix}$
TX double output ICCII++	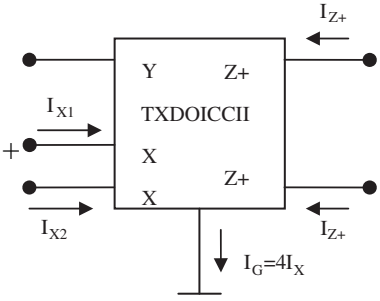	$\begin{bmatrix} V_{X1} \\ V_{X2} \\ I_Y \\ I_{Z+} \\ I_{Z+} \end{bmatrix} = \begin{bmatrix} 0 & 0 & -1 & 0 & 0 \\ 0 & 0 & -1 & 0 & 0 \\ 0 & 0 & 0 & 0 & 0 \\ 1 & 0 & 0 & 0 & 0 \\ 0 & 1 & 0 & 0 & 0 \end{bmatrix} \begin{bmatrix} I_{X1} \\ I_{x2} \\ V_Y \\ V_{Z+} \\ V_{Z+} \end{bmatrix}$
TX double output ICCII−− (floating)	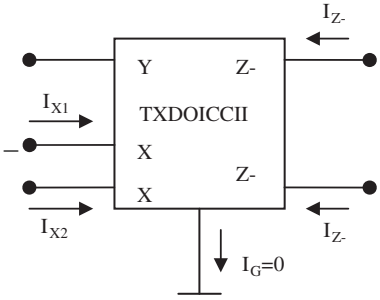	$\begin{bmatrix} V_{X1} \\ V_{X2} \\ I_Y \\ I_{Z-} \\ I_{Z-} \end{bmatrix} = \begin{bmatrix} 0 & 0 & -1 & 0 & 0 \\ 0 & 0 & -1 & 0 & 0 \\ 0 & 0 & 0 & 0 & 0 \\ -1 & 0 & 0 & 0 & 0 \\ 0 & -1 & 0 & 0 & 0 \end{bmatrix} \begin{bmatrix} I_{X1} \\ I_{x2} \\ V_Y \\ V_{Z-} \\ V_{Z-} \end{bmatrix}$

Table VI represents the TXBOICCII realized from an ICCII+ and an ICCII− with a common *Y* terminal. The TXDOICCII++ realized from two ICCII+, with a common *Y* terminal, is also given in Table VI.

The TXDOICCII−− realized from two ICCII− with a common *Y* terminal is also given in Table VI. In this realization the current $I_G = 0$ and it is seen that this results in the property of having floating realization of the TXDOICCII−−, which is not possible to obtain with single *X* DOICCII−− realization.

Figure 4(a) represents the new pathological representation of the TXBIOCCII, which includes two VM, one norator and one CM.

Figure 4(b) represents the new pathological representation of the TXDOICCII++, which includes two VM and two CM.

Figure 4(c) represents the new pathological representation of the floating TXDOICCII−−, which includes two VM and two norators only.

Table VII includes a summary showing the number of pathological elements plus grounded resistors if any in each of the two-output CCII and ICCII family.

4. EXAMPLES

Two examples are considered in the section. The first example is for current mode oscillators using DOCCII and BOCCII and is based on the first two realizations given in Table IV. The second

DOI: 10.1002/cta

Table VI. Realization of two *X* two-output ICCII family members using two single-output ICCII.

TX two-output ICCII	Block diagram realization using two single-output ICCII
TXBOICCII using a ICCII+ and a ICCII−	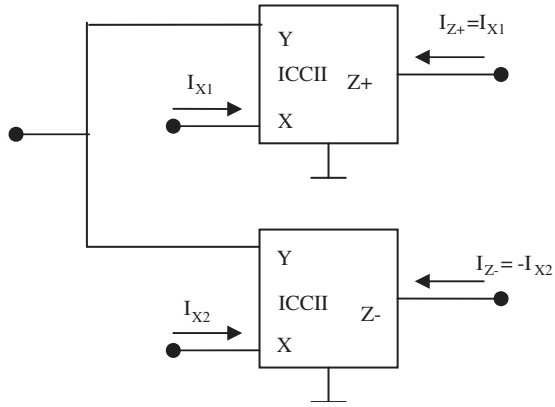
TXDOICCII++ using two ICCII+	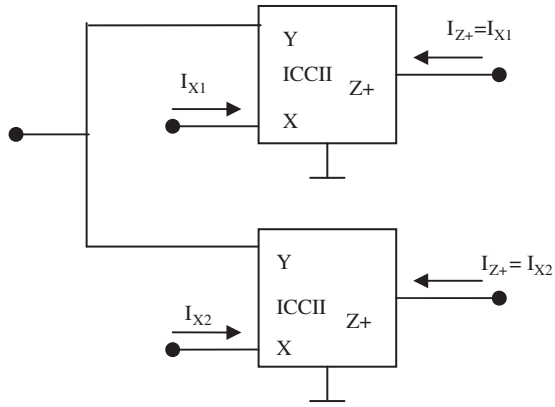
TXDOICCII−− using two ICCII−	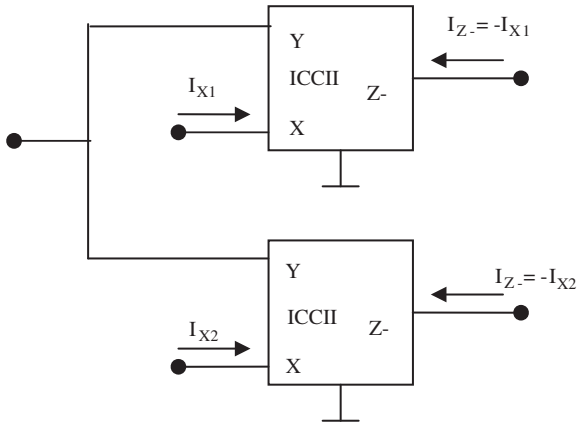

DOI: 10.1002/cta

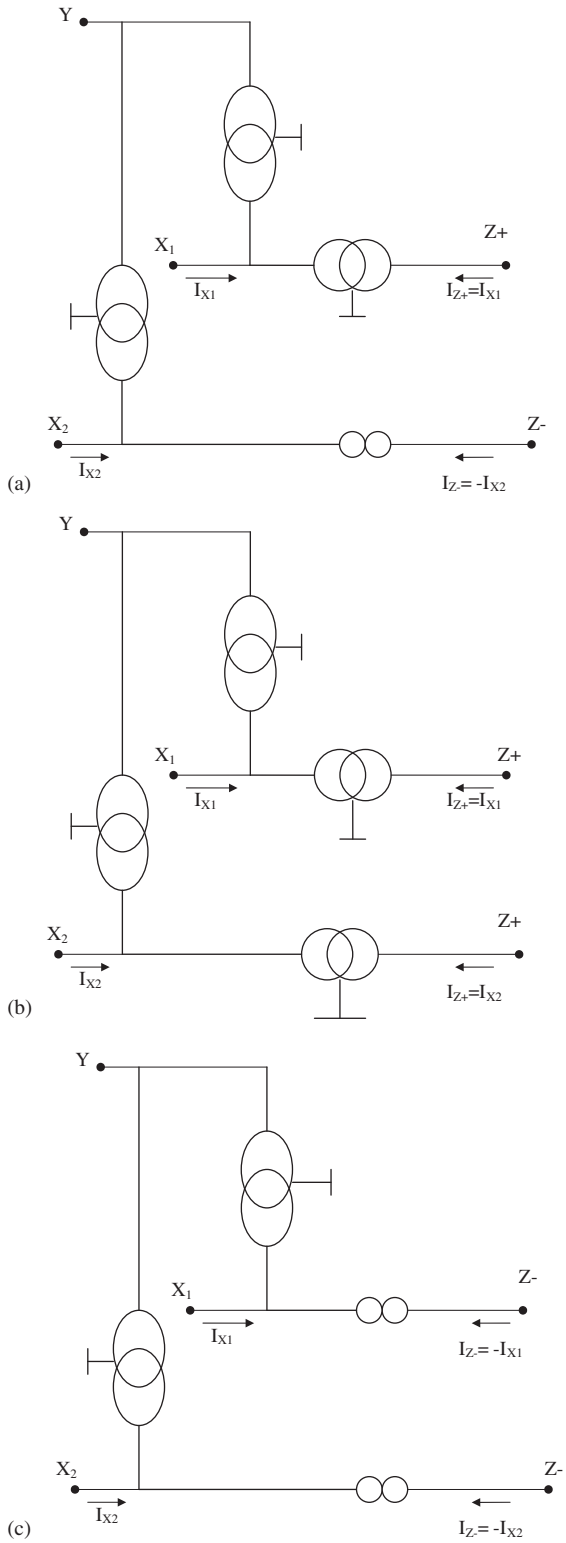

Figure 4. (a) Pathological representation of two X balanced output ICCII; (b) pathological representation of two X DOICCII$++$; and (c) pathological representation of two X DOICCII$--$.

DOI: 10.1002/cta

Table VII. Summary of the elements used in the pathological representations of the two-output CCII and ICCII family members.

No.	Element	VM	CM	Nullator	Norator	Resistor	Ref.	Fig.
1	BOCCII	0	0	4	4	5	13	
2	DOCCII++	0	0	3	3	3	13	
3	DOCCII−−	0	0	5	5	7	13	
4	BOICCII	0	0	5	5	7	New	
5	DOICCII++	0	0	4	4	5	New	
6	DOICCII−−	0	0	6	6	9	New	
7	BOCCII	0	2	2	0	0	9	1(a)
8	DOCCII++	0	3	3	0	0	New	1(b)
9	DOCCII−−	0	2	2	0	0	New	1(c)
10	BOICCII	1	2	1	0	0	New	2(a)
11	DOICCII++	1	3	2	0	0	New	2(b)
12	DOICCII−−	1	2	1	0	0	New	2(c)
13	TXBOCCII	0	1	2	1	0	New	3(a)
14	TXDOCCII++	0	2	2	0	0	New	3(b)
15	TXDOCCII−−	0	0	2	2	0	New	3(c)
16	TXBOICCII	2	1	0	1	0	New	4(a)
17	TXDOICCII++	2	2	0	0	0	New	4(b)
18	TXDOICCII−−	2	0	0	2	0	New	4(c)

example is for a current mode low-pass filter using a BOICCII and is based on the first realization given in Table VI.

4.1. Current mode oscillators

To demonstrate the importance of the pathological representation of active circuits, which results in the generation of new circuits ideally equivalent to each other, the following example is considered in details.

The grounded passive elements oscillator shown in Figure 5(a) was introduced in [17] and it employs a DOCCII and a BOCCII. Figure 5(b) represents the equivalent four single-output CCII oscillator circuit with the DOCCII++ replaced by two single-output, CCII+ and the BOCCII is replaced by a single-output CCII+ and a single-output CCII−.

To simplify the pathological representation of this oscillator circuit and to generate the family of equivalent oscillator circuits, the fourth single-output CCII+ delivering the output current is not included. The two resistors R_1 at the two X terminals of CCII+ number 1 and 2 at nodes 3 and 5 are taken equally. This will not provide any inconvenience in tuning as will be explained later. The circuit of Figure 6(a) is equivalent to that of Figure 5(a) and has the same state matrix equation given by

$$\begin{bmatrix} \dfrac{dv1}{dt} \\ \dfrac{dv2}{dt} \end{bmatrix} = \begin{bmatrix} \dfrac{1}{C_1}\left(\dfrac{1}{R_1}-\dfrac{1}{R}\right) & -\dfrac{1}{C_1R_2} \\ \dfrac{1}{C_2R_1} & 0 \end{bmatrix} \begin{bmatrix} v_1 \\ v_2 \end{bmatrix} \tag{1}$$

The condition of oscillation is given by

$$R = R_1 \tag{2}$$

The condition of oscillation should be controlled by varying R instead of varying the two equal resistors R_1.

The radian frequency of oscillation is given by

$$\omega_o = \frac{1}{\sqrt{C_1C_2R_1R_2}} \tag{3}$$

Similarly, the frequency of oscillation should be controlled by R_2 instead of varying the two equal resistors R_1.

DOI: 10.1002/cta

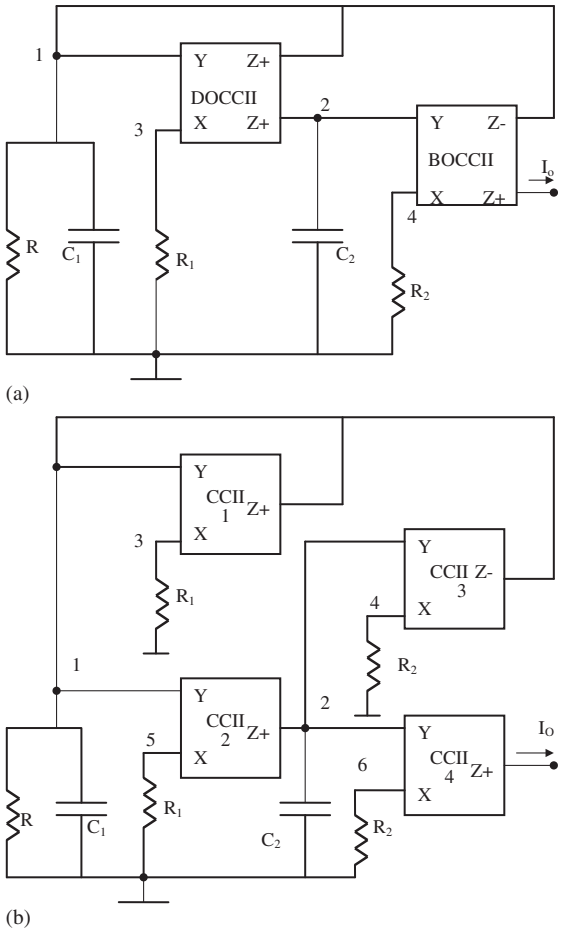

Figure 5. (a) Two-output CCII grounded passive elements oscillator [17] and (b) four single-output CCII equivalent circuit to Figure 5(a).

Sixteen alternative pathological mirror nullor representations resulting in ideally equivalent oscillator circuits to that of Figure 6(a) are possible as summarized in Table VIII. Eight of the generated oscillator circuits are related to the other eight by the adjoint network theorem. The pathological representation of the circuit of Figure 6(a) is given in Figure 6(b). An interesting feature of two of the new circuits numbers 15 and 16 in Table VIII is that they have floating property since $I_G = 0$. Owing to limited space, only the pathological mirror nullor representations of these two circuits are given in Figures 6(c) and (d). It should be noted that the circuit shown in Figure 6(c) employs a TXDOICCII$--$ and a CCII$-$.

4.2. Current mode low-pass filters

The second practical example is for a current mode low-pass filter using two ICCII. Based on the transformations discussed in the paper, an equivalent current mode low-pass filter using BOICCII is given.

The importance of the transformation of a two single-output ICCII to a BOICCII is demonstrated by the following example on current mode low-pass filter. Several current mode filters are available in the literature realizing different types of transfer functions [18–25].

Consider the two ICCII+ current mode filter shown in Figure 7(a) [20].

The current transfer function is given by

$$\frac{\mathrm{IL_P}}{\mathrm{I_I}} = \frac{1}{s^2 C_1 C_2 R_1 R_2 + s(C_1 + C_2)R_2 + 1} \tag{4}$$

DOI: 10.1002/cta

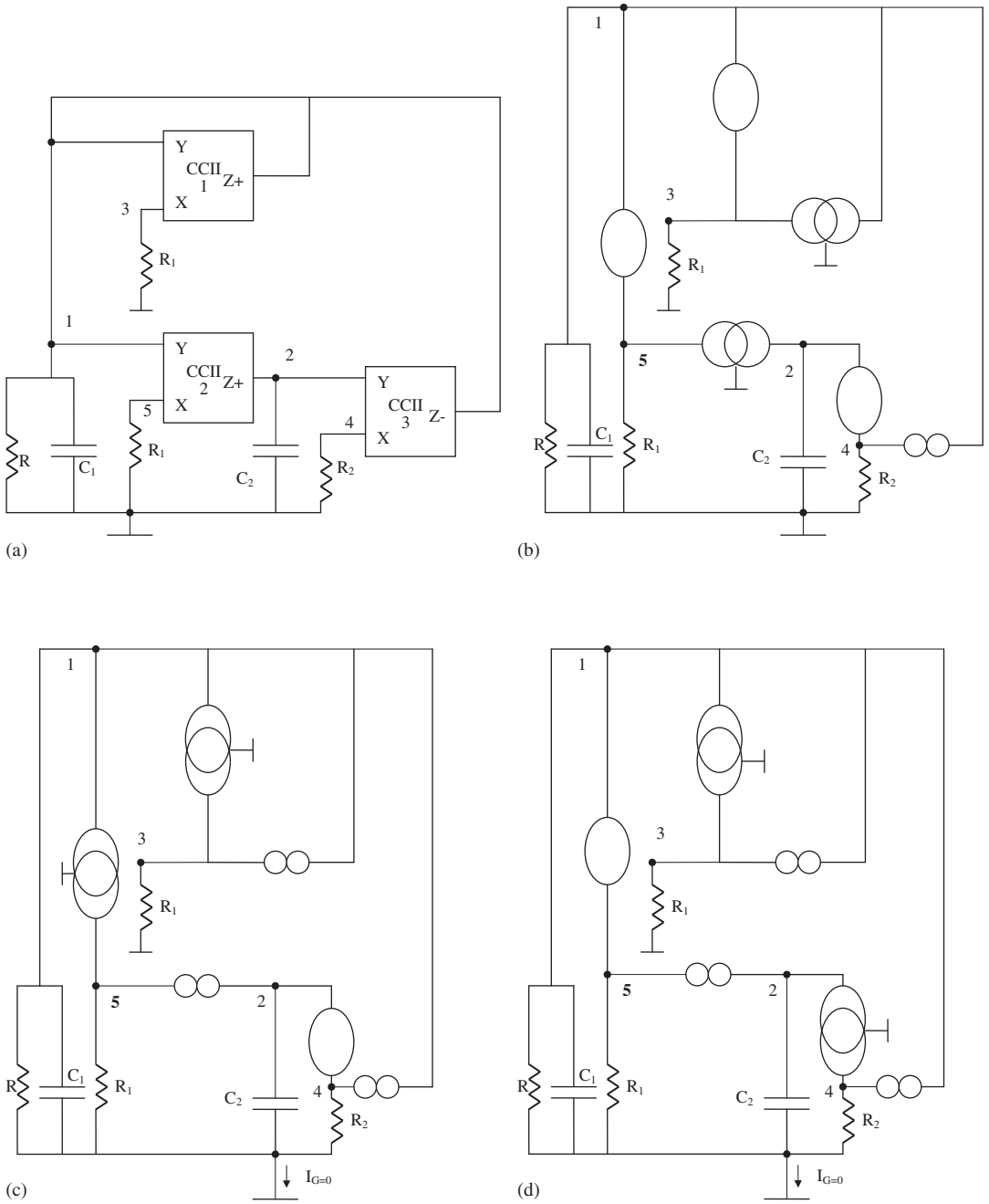

Figure 6. (a) Simplified three single-output CCII oscillator circuit; (b) pathological modeling of the circuit of Figure 6(a); (c) circuit 15 in Table VIII equivalent circuit to Figure 6(a); and (d) circuit 16 in Table VIII equivalent circuit to Figure 6(a).

The ω_o and Q are given by

$$\omega_o = \frac{1}{\sqrt{C_1 C_2 R_1 R_2}} \tag{5}$$

$$Q = \frac{1}{(C_1 + C_2)} \sqrt{\frac{C_1 C_2 R_1}{R_2}} \tag{6}$$

DOI: 10.1002/cta

Table VIII. Sixteen equivalent realizations to the oscillator circuit of Figure 6(a).

Circuit number	Conveyor 1	Conveyor 2	Conveyor 3	Reference
1	CCII+	CCII+	CCII−	16
2	CCII+	CCII−	CCII+	New
3	CCII+	CCII+	ICCII+	New
4	CCII+	ICCII+	CCII+	New
5	ICCII−	ICCII+	CCII+	New
6	ICCII−	CCII−	CCII+	New
7	ICCII−	CCII+	ICCII+	New
8	ICCII−	CCII+	CCII−	New
9	CCII+	CCII−	ICCII−	New
10	CCII+	ICCII+	ICCII−	New
11	CCII+	ICCII−	CCII−	New
12	CCII+	ICCII−	ICCII+	New
13	ICCII−	ICCII−	ICCII+	New
14	ICCII−	ICCII+	ICCII−	New
15	ICCII−	ICCII−	CCII−	New
16	ICCII−	CCII−	ICCII−	New

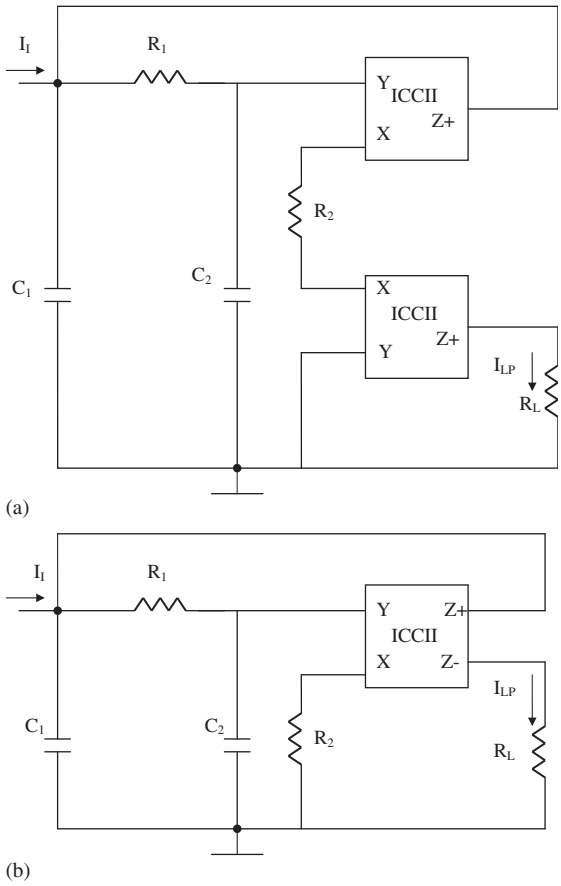

Figure 7. (a) Current mode low-pass filter using two ICCII and (b) current mode low-pass filter using balanced output ICCII.

The parasitic parameters are affecting the above equations since they are affecting C_1 and R_2 as follows:

$$C_{1a} = C_1 + C_{Z1} \tag{7}$$

DOI: 10.1002/cta

$$C_{2a} = C_2 + C_{Y1} \tag{8}$$

$$R_{2a} = R_2 + R_{X1} + R_{X2} \tag{9}$$

Transformation of the two $ICCII+$ circuit of Figure 7(a) results in the equivalent current mode circuit shown in Figure 7(b) having the same Equations (4)–(8). Equation (9), however, will be modified as follows:

$$R_{2a} = R_2 + R_X \tag{10}$$

It is seen that the parasitic elements are having less effect on the BOICCII current mode circuit. To confirm the above analysis, simulation results are carried out using the differential voltage current conveyor (DVCC) CMOS circuit shown in Figure 8 [26, 27]. The transistor aspect ratios for the DVCC circuit are given in Table IX based on the 0.5 μm CMOS model from MOSIS. The supply voltages used are ± 1.5 V and $V_{B1} = -0.52$ V and $V_{B2} = 0.33$ V.

Simulation results are given next based on the equal C design, for which the design equations for R_1 and R_2 are given by

$$R_1 = \frac{2Q}{\omega_0 C} \quad \text{and} \quad R_2 = \frac{1}{2Q\omega_0 C} \tag{11}$$

Figure 9(a) represents the magnitude and the phase characteristics together with the ideal response of the circuit of Figure 7(a) designed to have a cutoff frequency of 1 MHz and $Q = 0.707$.

The circuit design parameters taken are $C_1 = C_2 = 100$ pF, $R_1 = 2.25\,\text{k}\Omega$ and $R_2 = 1.125\,\text{k}\Omega$.

Figure 9(b) represents the magnitude and the phase characteristics together with the ideal response of the circuit of Figure 7(b) designed for the same values as above.

It is seen that the circuit of Figure 7(b) is less affected by parasitic parameters and has better frequency response.

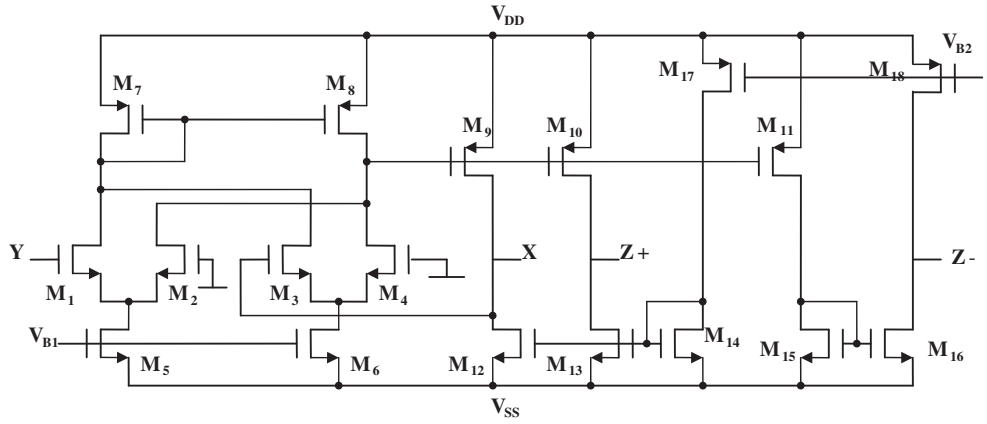

Figure 8. CMOS of balanced output ICCII [26].

Table IX. Dimensions of the MOS Transistors of Figure 8.

MOS Transistors	$W(\mu\text{m})/L(\mu\text{m})$
M_1, M_2, M_3 and M_4	$\frac{2.5}{1}$
M_5 and M_6	$\frac{8}{1}$
M_{12}, M_{13}, M_{14}, M_{15} and M_{16}	$\frac{20}{2.5}$
M_7 and M_8	$\frac{10}{1}$
M_9, M_{10}, M_{11}, M_{17} and M_{18}	$\frac{40}{2}$

DOI: 10.1002/cta

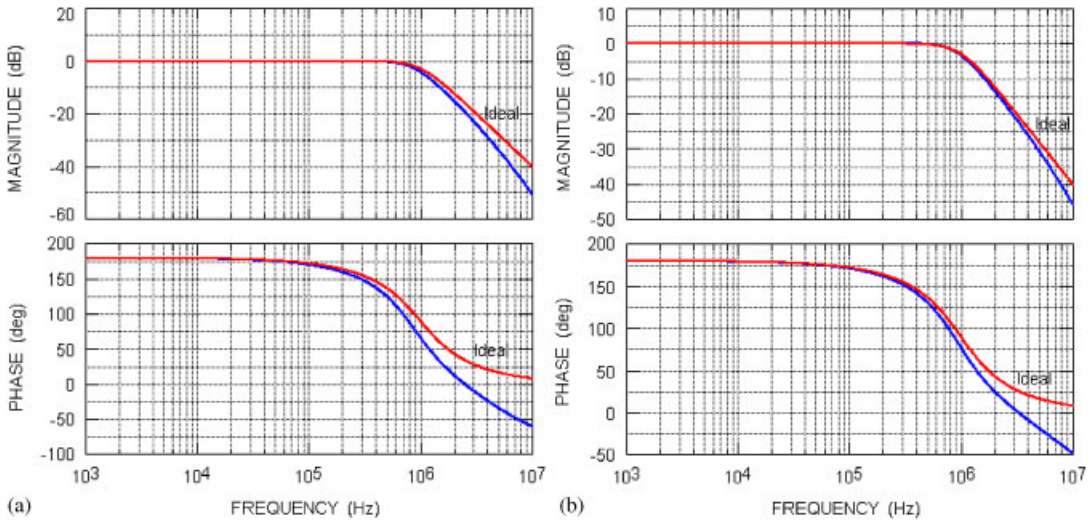

Figure 9. (a) Low-pass frequency response of the two ICCII circuit and (b) low-pass frequency response of the BOICCII circuit.

Simulation results prove that the response of the second circuit shown in Figure 9(b) is better than the response shown in Figure 9(a). Although the two circuits are ideally equivalent, the circuit of Figure 7(a) has R_2 increased to R_2+2R_X due to the parasitic resistances of the two ICCII.

The circuit of Figure 7(b) has R_2 increased to R_2+R_X due to the parasitic resistance of the BOICCII.

This example demonstrates clearly that the generation of one circuit based on the modeling to another ideally equivalent circuit is very useful in obtaining a better performance circuit in the actual case.

5. CONCLUSIONS

The pathological mirror elements [28, 29] and nullor representation of the two-output current conveyor family is given. New nullator norator resistors' representation of the missing members of the two-output current conveyor family is compared in Table VII with the pathological mirror and nullor representation. Simplified representations of the two-output current conveyors based on using two single-output current conveyors is given and illustrated by two examples. The first example is for a transformation of a two-output CCII current mode oscillator to a family of oscillators using single-output CCII and ICCII. It is found that there are 16 equivalent oscillator circuits using combinations of single-output CCII or ICCII as summarized in Table VIII. It is worth noting that eight of them are related to the other eight by the adjoint network theorem.

The CCII and ICCII are completing each other in obtaining a set of ideally equivalent circuits. The practical differences will depend on the CMOS circuit used.

It should be noted that the combination of both CCII and ICCII may result in circuits with some unique properties than cannot be achieved with CCII alone or with ICCII alone.

Consider the circuit numbers 15 and 16 described in Table VIII and shown in Figures 6(c) and (d), each employ one CCII− and two ICCII−. They are the only two floating circuits among the 16 equivalent circuits.

This unique feature cannot be achieved with CCII alone or with ICCII alone. Thus, it is important to appreciate the advantages obtained in combining CCII and ICCII in some circuit applications.

Of course, the transformations considered in this paper can be used both ways and the second example is for the transformation of two single-output ICCII current mode low-pass filter into an equivalent BOICCII current mode low-pass filter. In the actual case, the two circuits are slightly different due to parasitic elements as demonstrated by analysis and by simulations.

DOI: 10.1002/cta

REFERENCES

1. Carlin HJ. Singular network elements. *IEEE Transactions on Circuit Theory* 1964; **11**:67–72.
2. Svoboda JA. Current conveyors, operational amplifiers and nullors. *IEE Proceedings* Part G 1989; **136**: 317–322.
3. Grimbleby JB. Symbolic analysis of networks containing current conveyors. *Electronics Letters* 1992; **28**: 1401–1403.
4. Awad IA, Soliman AM. Inverting second generation current conveyors: the missing building blocks, CMOS realizations and applications. *International Journal of Electronics* 1999; **86**:413–432.
5. Awad IA, Soliman AM. On the voltage mirrors and the current mirrors. *Analog Integrated Circuits and Signal Process* 2002; **32**:79–81.
6. Haigh DG, Tan FQ, Papavassiliou C. Systematic synthesis of active-RC circuit building-blocks. *Analog Integrated Circuits and Signal Process* 2005; **43**:297–315.
7. Haigh DG, Clarke TJW, Radmore PM. Symbolic framework for linear active circuits based on port equivalence using limit variables. *IEEE Transactions on Circuits Systems I* 2006; **53**:2011–2024.
8. Saad RA, Soliman AM. Use of mirror elements in the active device synthesis by admittance matrix expansion. *IEEE Transactions on Circuits Systems I* 2008; **55**:2726–2735.
9. Saad RA, Soliman AM. A new approach for using the pathological mirror elements in the ideal representation of active devices. *International Journal of Circuit Theory and Applications*, 2008. DOI: 10.1002/cta.534.
10. Bruun E. Constant bandwidth current mode operational amplifier. *Electronics Letters* 1991; **27**:1673–1674.
11. Elwan HO, Soliman AM. A novel CMOS current conveyor realization with an electronically tunable current mode filter suitable for VLSI. *IEEE Transactions on Circuits and Systems II* 1996; **43**:663–670.
12. Horng JW, Hou CL, Chang CM. Multi-input differential current conveyor, CMOS realization and application. *IET Circuits*, *Devices and Systems* 2008; **2**:469–475.
13. Tlelo-Cuautle E, Sanchez-Lopez C, Moro-Fr´as D. Symbolic analysis of (MO) (I)CCI(II)(III)-based analog circuits. *International Journal of Circuit Theory and Applications* 2009; DOI: 10.1002/cta.582.
14. El-Adawy AA, Soliman AM, Elwan HO. A novel fully differential current conveyor and applications for analog VLSI. *IEEE Transactions on Circuits and Systems II* 2000; **47**:306–313.
15. Sobhy EA, Soliman AM. Realization of fully differential voltage second generation current conveyor with an application. *International Journal of Circuit Theory and Applications*, 2008; DOI: 10.1002/566.
16. Soliman AM. Synthesis of grounded capacitor and grounded resistor oscillators. *Journal of Franklin Institute* 1999; **336**:735–746.
17. Soliman AM. Current mode CCII oscillators using grounded capacitors and resistors. *International Journal of Circuit Theory and Applications* 1998; **26**:431–438.
18. Soliman AM. Current mode filters using two output inverting CCII. *International Journal of Circuit Theory and Applications* 2008; **36**:875–881.
19. Souliotis G, Haritantis I. Current-mode filters based on current mirror arrays. *International Journal of Circuit Theory and Applications* 2008; **36**:173–183.
20. Soliman AM. The CCII+ and the ICCII as basic building blocks in low-pass filter realizations. *International Journal of Circuit Theory and Applications* 2008; **36**:493–509.
21. Desai M, Aronhime P. Current mode synthesis using node expansion techniques. *Analog Integrated Circuits and Signal Processing* 1994; **6**:255–263.
22. Horng JW, Hou CL, Chang CM, Chou HP, Lin CT. High input impedance voltage mode universal filter with one input and five outputs using current conveyors. *Circuits Systems and Signal Processing* 2006; **25**:767–777.
23. Higashimura M. Current mode transfer function using CCIIs with grounded passive elements. *IEICE Transitions* 1991; **74**:1017–1019.
24. Hwang YS, Wu DS, Chen JJ, Shih CC, Chou WS. Design of current-mode MOSFET-C filters using OTRAs. *International Journal of Circuit Theory and Applications* 2008; **36**:397–411.
25. Soliman AM. Current mode universal filters using current conveyors: classification and review. *Circuits Systems and Signal Processing* 2008; **27**:405–427.
26. Elwan HO, Soliman AM. Novel CMOS differential voltage current conveyor and its applications. *IEE Proceedings—Circuits*, *Devices and Systems* 1997; **144**:195–200.
27. Chiu W, Liu SI, Tsao HW, Chen JJ. CMOS differential difference current conveyors and their applications. *IEE Proceedings—Circuits*, *Devices and Systems* 1996; **143**:91–96.
28. Soliman AM. Saad RA. The voltage mirror current mirror pair as a universal element. *International Journal of Circuit Theory and Applications* 2009; DOI: 10.1002/cta.596.
29. Saad RA, Soliman AM. On the systematic synthesis of CCII based floating simulators. *International Journal of Circuit Theory and Applications* 2009; DOI: 10.1002/cta.604.